

# Substituent effect of group 14 elements on the ring-opening reaction of cyclobutene†

Munehiro Hasegawa, Ippei Usui, Soichiro Konno and Masahiro Murakami\*

Received 8th April 2010, Accepted 9th June 2010

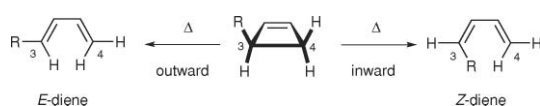
First published as an Advance Article on the web 28th July 2010

DOI: 10.1039/c004972g

A series of cyclobutenes bearing group 14 elements at the 3-position were synthesized, and their thermal ring-opening reactions were studied. Carbon-substituted cyclobutene underwent the ring-opening reaction through an outward pathway to afford the *E*-diene exclusively. On the other hand, the ring-opening reaction of the silyl, germyl, and stannyl substituted cyclobutenes occurred in both outward and inward directions giving a mixture of *E* and *Z* isomers. The structural features of the calculated transition state and population analysis suggested that the formation of the *Z*-isomer could be ascribed to the donor/acceptor interaction between the HOMO and the  $\sigma^*$  orbital of group 14 elements. Interestingly, the order of inward preference was Si > Sn > Ge. These rotational behaviors of silyl, germyl, and stannyl substituents were explained by taking into account the energy gap and the magnitude of overlap between the  $\sigma^*$  orbital and HOMO.

## 1. Introduction

The thermal ring-opening reaction of cyclobutenes to produce 1,3-butadienes is one of the most fundamental electrocyclic reactions. It presents a typical example which obeys the Woodward–Hoffmann rules.<sup>1</sup> Nonetheless, the rules allow two rotational options for a substituent located at the 3-position of cyclobutene (Scheme 1); the 3-substituent can move either in an inward direction to afford *Z*-buta-1,3-diene or in an outward direction to give *E*-buta-1,3-diene (the structures of the produced dienes are drawn in an *s-cis* conformation for convenience throughout this manuscript).



**Scheme 1** Torquoselection in a thermal ring-opening reaction of 3-substituted cyclobutene

The selectivity with regard to the rotational direction was named as torquoselectivity by Houk, and has been extensively studied since the 1980's.<sup>2</sup> The inward rotation is generally disfavored under thermal conditions because of steric repulsion which develops between the rotating 3-substituent and the opening cyclobutene framework. For instance, the ring-opening reaction of 3-methylcyclobutene selectively produces (*E*)-penta-1,3-diene *via* outward rotation.<sup>3</sup>

Contrary to the expectation based on steric grounds, however, electron-withdrawing substituents such as a formyl group prefer inward rotation to outward rotation.<sup>2c</sup> Rondan and Houk explained the contrasteric rotational behavior of electron-withdrawing substituents on the basis of orbital interaction

Department of Synthetic Chemistry and Biological Chemistry, Kyoto University, Katsura, Kyoto, 615-8510, Japan. E-mail: murakami@sbchem.kyoto-u.ac.jp; Fax: +81 (75) 383-2748

† Electronic supplementary information (ESI) available: Details of the kinetic experiment and optimized geometries of stationary points as Cartesian coordinates. See DOI: 10.1039/c004972g

theory.<sup>2a–2c</sup> When a formyl group rotates inward and reaches a transition state, the formyl group and the opening cyclobutene skeleton are close enough to invoke intramolecular donor/acceptor orbital interaction (Fig. 1); the vacant  $\pi^*$  orbital of the formyl group accepts electron density from the HOMO of the cyclobutene skeleton, which is a C3–C4  $\sigma$ -bond half-breaking by conrotation. This electron delocalization stabilizes the inward transition state. On the other hand, an analogous stabilization is unavailable at the transition state of outward rotation, in which the electron-accepting  $\pi^*$  orbital is getting more distant from the HOMO. Thus, the contrasteric behavior of electron-withdrawing substituents can be explained on electronic grounds.

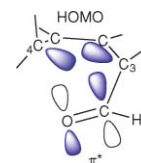
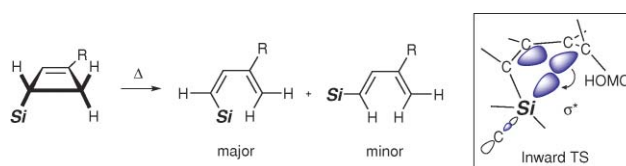


**Fig. 1**  $\pi^*$ -HOMO interaction of the inward transition state.

We have reported that a silyl substituent prefers inward rotation rather than outward rotation despite its sterically demanding nature (Scheme 2).<sup>4,5</sup> The preference for inward rotation can be understood on the basis of the Rondan and Houk's theory; the antibonding  $\sigma^*$  orbital of an Si–C linkage is energetically low-lying, and thus, acts as the acceptor accommodating electron density from the HOMO of the cyclobutene skeleton, like the vacant  $\pi^*$  orbital of a formyl group.<sup>6,7</sup>



**Scheme 2** Ring-opening reaction of 3-silylcyclobutenes

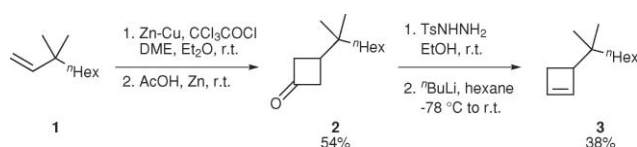
Substituents of group 14 elements other than silicon, such as germyl and stannyl substituents, also carry low-lying  $\sigma^*$  orbitals which can accept electron density from a donor orbital if present in its proximity. Therefore, those substituents are expected to show a preference for inward rotation like silyl substituents.<sup>8</sup> In addition, the energy levels of their  $\sigma^*$  orbitals are even lower than that of a Si–C  $\sigma^*$  orbital.<sup>9</sup> In this regard, orbital interaction theory expects a greater preference for inward rotation for the substituents of group 14 elements which are located below silicon in the periodic table. This simple expectation based on the previous study on 3-silylcyclobutene and orbital interaction theory should be confirmed by an experimental study.

Herein, we report the synthesis of a series of cyclobutenes having a structurally analogous substituent of group 14 elements at the 3-position and their rotational behaviors in the thermal ring-opening reaction are discussed.

## 2. Results

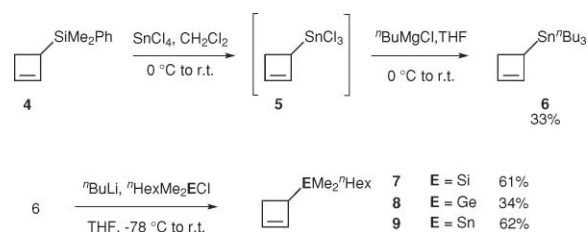
### Synthesis of substituted cyclobutenes

Initially, a series of cyclobutenes with the 3-carbon bonded to a group 14 element possessing otherwise identical structure were synthesized. Carbon analogue **3** was synthesized from 3,3-dimethylnon-1-ene **1** (Scheme 3). A [2 + 2] cycloaddition reaction of **1** with dichloroketene followed by dechlorination with zinc furnished cyclobutanone **2**. The cyclobutanone **2** was transformed to the corresponding tosylhydrazone, which was then subjected to the Shapiro reaction. Treatment with 2.2 equiv. of butyllithium followed by protonolysis with water furnished 3-(1,1-dimethylheptyl)cyclobutene **3**.



**Scheme 3** Synthesis of 3-(1,1-dimethylheptyl)cyclobutene **3**

3-(Phenyldimethylsilyl)cyclobutene **4** was synthesized according to a procedure we previously reported;<sup>10</sup> a [2 + 2] cycloaddition of dimethylphenylvinylsilane with dichloroketene followed by a dechlorination reaction with Zn–Cu couple afforded 3-(dimethylphenylsilyl)cyclobutanone, which was then transformed to the corresponding tosylhydrazone. The tosylhydrazone was subjected to the Shapiro reaction and the subsequent hydrolysis with water afforded 3-(phenyldimethylsilyl)cyclobutene **4**. The silicon atom of **4** was then replaced with tin on treatment with  $\text{SnCl}_4$ <sup>11</sup> and the subsequent per-alkylation reaction with an excess amount of butylmagnesium chloride afforded 3-(tributylstannyl)cyclobutene **6**. Treatment of **6** with butyllithium brought about tin–lithium exchange to generate cyclobutenyllithium. Substitution reactions with electrophilic metal chlorides successfully introduced the desired group 14 elements equipped with the same alkyl substituents at the 3-position and cyclobutenes **7–9** were obtained in 61%, 34%, and 62% yields, respectively (Scheme 4).

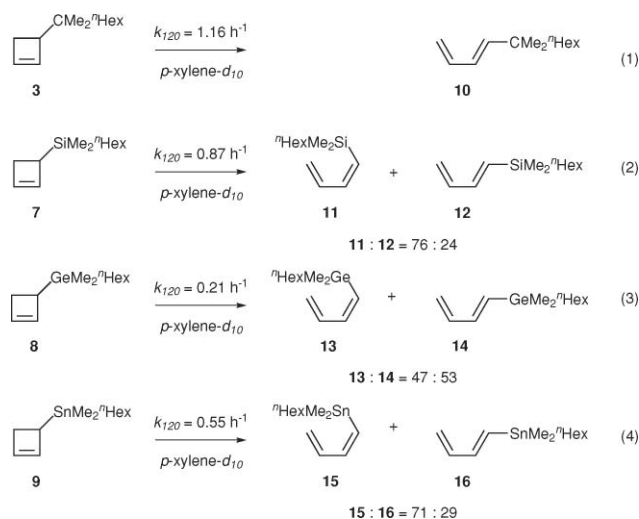


**Scheme 4** Synthesis of cyclobutenes having a substituent of group 14 elements

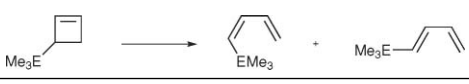
### Thermal ring-opening reaction

The ring-opening reactions of cyclobutenes **3** and **7–9** were carried out in *p*-xylene-*d*<sub>10</sub> in an NMR tube at 120 °C, and the progress of the reaction was monitored by NMR measurements. In the reaction of 3-(dimethylhexylstannyl)cyclobutene **9**, galvinoxyl free radical was added to the reaction mixture in order to prevent geometrical isomerization of the produced dienes by a radical pathway.

As shown in Scheme 5, carbon-substituted cyclobutene **3** underwent the ring-opening reaction through an outward pathway to afford the *E*-diene **10** exclusively. On the other hand, ring-opening of the other substituted cyclobutenes **7–9** occurred in both outward and inward directions giving a mixture of *E* and *Z* isomers. The silyl substituent preferred inward rotation over outward rotation by a ratio of 76:24. The stannyl substituent also rotated preferentially in an inward direction with a ratio of 71:29. These results obtained with **7** and **9** are in good agreement with the results of our previous studies,<sup>4a,8</sup> confirming the inward preferences of the silyl and stannyl substituents. In contrast to the silicon and tin analogues which exhibited considerable preference for inward rotation over outward rotation, the germanium analogue **8** barely showed selectivity to afford a mixture of almost equimolar amounts of *Z* and *E* isomers (*Z*:*E* = 47:53). Furthermore, the reaction of **8** was significantly slower than those of the others. Germanium is placed between silicon and tin in the periodic table. Nevertheless, its rotational behavior observed failed to follow an extrapolative expectation made on the basis of rotational behaviors of silicon and tin analogues.



**Scheme 5** Ring-opening reaction of 3-substituted cyclobutenes

**Table 1** Calculated activation energies (kcal/mol) and *Z/E* ratios of the ring-opening reaction of **17–19**


Cyclobutene	EMe <sub>3</sub>	ΔE <sub>in</sub> <sup>‡</sup>	ΔE <sub>out</sub> <sup>‡</sup>	ΔΔE <sub>in-out</sub> <sup>‡</sup>	<i>Z:E</i>	
					calc <sup>a</sup>	exp <sup>b</sup>
17	SiMe <sub>3</sub>	29.9	30.8	-0.94	77:23	76:24
18	GeMe <sub>3</sub>	31.1	31.0	0.09	47:53	47:53
19	SnMe <sub>3</sub>	30.1	30.7	-0.66	69:31	71:29

<sup>a</sup> Predicted at 120 °C. <sup>b</sup> Observed at 120 °C.

### 3. Computational results

Theoretical calculation was carried out on the ring-opening reaction employing 3-(trimethylsilyl)cyclobutene **17**,<sup>6</sup> 3-(trimethylgermyl)cyclobutene **18**, and 3-(trimethylstannyl)cyclobutene **19** as the prototype model.<sup>12,13</sup>

#### 3.1. Activation energies

The calculated activation energies of the ring-opening reaction are shown in Table 1. In both cases of 3-silylcyclobutene **17** and 3-stannylcyclobutene **19**, the activation energy of inward rotation is distinctly smaller than that of outward rotation; the inward/outward energy difference is -0.94 kcal/mol for **17** and -0.66 kcal/mol for **19**,<sup>14</sup> respectively. On the other hand, the inward and outward transition states are of approximately the same energy as 3-germylcyclobutene **18**. Thus, the *Z:E* ratios estimated based on calculated energy differences between inward and outward transition states accord well with those experimentally observed at 120 °C.

#### 3.2. Transition state structures

Rough sketches of the calculated structures of the inward and outward transition states of **17–19** are shown in Fig. 2, and the representative geometrical parameters are listed in Table 2.

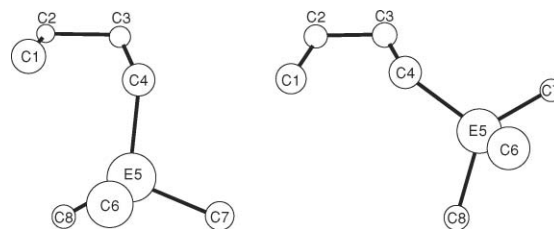
**3-Silylcyclobutene 17.** There are three methyl carbons (C6, C7, and C8) bound to the central silicon atom Si5. In the ground state, there is little difference between three Si-CH<sub>3</sub> linkages. The distances of Si-C6, Si-C7, and Si-C8 are 1.891 Å, 1.892 Å, and 1.890 Å, respectively. In the inward transition state, the Si5-

**Table 2** Geometrical parameters of 3-substituted cyclobutenes<sup>a</sup>

Cyclobutene	E	Transition state	E5-C6	E5-C7	E5-C8	∠C1C4E5C7
			Å	Å	Å	
17	Si	cyclobutene	1.891	1.892	1.890	
		inward TS	1.891	1.898	1.886	170.3
		outward TS	1.889	1.893	1.892	132.4
18	Ge	cyclobutene	1.978	1.978	1.976	
		inward TS	1.975	1.983	1.971	170.2
		outward TS	1.975	1.978	1.977	130.0
19	Sn	cyclobutene	2.154	2.153	2.151	
		inward TS	2.151	2.158	2.145	171.2
		outward TS	2.151	2.153	2.153	132.3

<sup>a</sup> Distances are shown in Å and dihedral angles in degrees.**Table 3** Electron occupancy of σ/σ\* orbital of ring-opening reaction of 3-substituted cyclobutene from NBO analysis

Cyclobutene	E	Transition state	E5-C6	E5-C7	E5-C8
			σ/σ*	σ/σ*	σ/σ*
17	Si	cyclobutene	1.982/0.026	1.982/0.026	1.983/0.027
		inward TS	1.980/0.035	1.974/0.042	1.982/0.028
		outward TS	1.983/0.025	1.979/0.026	1.980/0.031
18	Ge	cyclobutene	1.976/0.031	1.976/0.030	1.978/0.031
		inward TS	1.975/0.037	1.969/0.044	1.976/0.032
		outward TS	1.977/0.030	1.973/0.030	1.974/0.033
19	Sn	cyclobutene	1.968/0.033	1.968/0.032	1.970/0.032
		inward TS	1.964/0.048	1.959/0.056	1.964/0.039
		outward TS	1.968/0.036	1.964/0.037	1.966/0.040

**Fig. 2** Geometries of inward TS and outward TS of 3-substituted cyclobutenes.

C7 distance is significantly longer than the Si5-C6 distance by 0.007 Å and the Si5-C8 distance by 0.012 Å. This result implies that the Si5-C7 linkage is specifically weakened. The dihedral angle C1-C4-Si5-C7 is 170.3°, suggesting that the half-breaking C1-C4 bond, around which HOMO electrons are distributed, eclipses well with the antibonding σ\* orbital of the Si5-C7 linkage. This structural feature fulfils the stereoelectronic demand for the HOMO distributed around the half-breaking C1-C4 linkage to act as an electron donor delocalizing its electron density into the σ\* Si5-C7 orbital. As a result of this electron delocalization into the σ\* orbital, the Si5-C7 linkage is weakened, and thus, elongated.

On the other hand, with the calculated outward transition state structure, the three Si-CH<sub>3</sub> distances fall in a narrower range, being suggestive of the paucity of analogous intramolecular donor/acceptor orbital interaction.

We next carried out the natural bond orbital (NBO) analysis to see the occupancy (Table 3).<sup>15,16</sup> Whereas three Si-CH<sub>3</sub> bonds have essentially the same occupancies of the σ orbitals and σ\* orbitals at the ground state, the occupancy of the Si5-C7 σ orbital at the inward transition state is lower than those of the Si5-C6 and Si5-C8 σ orbitals. On the contrary, the occupancy of the Si5-C7 σ\* orbital is higher than those of Si5-C6 and Si5-C8 σ\* orbitals. These results of the occupancy in the NBO analysis support our interpretation assuming the intramolecular donor/acceptor orbital interaction.

**3-Germylcyclobutene 18 and 3-stannylcyclobutene 19.** The structural features observed with the transition states of 3-germylcyclobutene **18** and 3-stannylcyclobutene **19** are analogous to those of 3-silylcyclobutene **17**. The Ge5-C7 linkage is longer than the Ge5-C6 and Ge-C8 linkages by 0.008 Å and 0.012 Å, respectively. The dihedral angle of C1-C4-Ge5-C7 is 170.2°. The Sn5-C7 bond length is also longer than those of the other two by 0.007 and 0.013 Å. The dihedral angles of C1-C4-Sn5-C7 is

171.2°. These calculated structural features of **18** and **19** suggest that the HOMO is distributed around the half-breaking C1–C4 linkage acts as an electron donor, delocalizing its electron density into the Ge5–C7 (or Sn5–C7)  $\sigma^*$  orbital.

## Discussion

There are two major factors which influence the magnitude of donor/acceptor orbital interaction. One is the energy difference of donor and acceptor orbitals and the other is their overlap. Proximity of donor and acceptor orbitals in energy results in better interaction. Lowering the energy level of an acceptor orbital reduces the energy difference to a donor orbital. The order of the energy level of the  $\sigma^*$  orbital is Si–C > Ge–C > Sn–C.<sup>9</sup> Thus, the order of the acceptor ability of the  $\sigma^*$  orbital in terms of the energy is Sn–C > Ge–C > Si–C (Fig. 3).

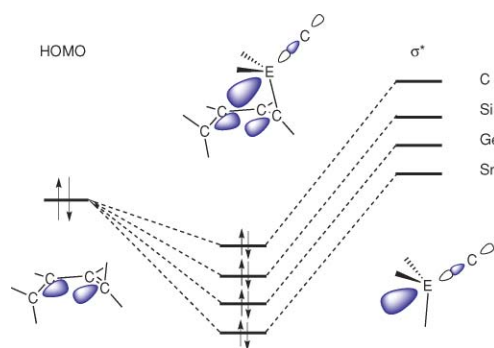


**Fig. 3** Orbital interaction between the  $\sigma^*$  orbital of group 14 elements and HOMO.

Better overlap of donor and acceptor orbitals also leads to better interaction. Carbon is more electronegative than the other group 14 elements. Whereas a  $\sigma$  orbital between carbon and a group 14 element is polarized toward carbon, its  $\sigma^*$  orbital is polarized outward on the group 14 element. The  $\sigma^*$  orbital of a more polarized  $\sigma$  bond is more broadly distributed on the electropositive end, increasing the potential of overlapping with an electron donor orbital. In most electronegativity scales, germanium is regarded to be more electronegative than silicon and tin.<sup>17</sup> In this respect, a Ge–C linkage can be considered to be less polarized than Si–C and Sn–C linkages. Thus, the acceptor ability of a Ge–C  $\sigma^*$  orbital is lower than those of the Si–C and Sn–C  $\sigma^*$  orbitals in terms of spatial distribution.

In addition, an interspatial distance between donor and acceptor orbitals should be also taken into account in evaluating the magnitude of the orbital overlap.<sup>8,18</sup> Fig. 4 shows the distances between the group 14 elements and the mid-points of the C1–C4 linkages, designated as M, in the inward transition states. Whereas

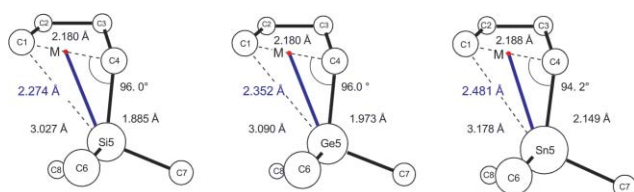


**Fig. 4** Calculated configuration of the group 14 elements and HOMO on the inward TS.

the Ge–M distance is longer than the Si–M distance by 0.078 Å, the Sn–M distance is significantly longer than the Si–M and Ge–M distances. Thus, the order of the interspatial distance between donor/acceptor orbitals is Sn–C  $\gg$  Ge–C > Si–C.

The rotational behaviors observed with a series of cyclobutenes possessing a group 14 substituent can be interpreted as follows on a qualitative basis. In contrast to the case of 3-alkylcyclobutene which exclusively gives the *E*-isomer *via* outward rotation, a force favoring inward rotation operates to furnish a mixture of stereoisomers in the cases of 3-silyl, 3-germyl-, and 3-stannylcyclobutenes. The origin of the contrastric force favoring inward rotation can be attributed to donor/acceptor orbital interaction between the  $\sigma^*$  orbital on the group 14 element and the HOMO of the cyclobutene skeleton. 3-Silylcyclobutene and 3-stannylcyclobutene exhibit similar torquoselectivities, which is explained by assuming that the factor in the energy level and the factor of the distance between the  $\sigma^*$  orbital and the HOMO cancel out in favoring inward ring-opening. The magnitude of inward preference of a germyl substituent is smaller than those of silicon and tin substituents, which is presumably because its electronegativity is closer to that of carbon than silicon and tin. The Ge–C  $\sigma^*$  orbital is less protruded in space than the Si–C  $\sigma^*$  orbital and Sn–C  $\sigma^*$  orbital, and thus can interact less effectively with the electron-donating HOMO.

## 4. Summary

We have prepared a series of cyclobutenes having a substituent of group 14 element substituent at the 3-position, and subjected them to a thermal ring-opening reaction to discuss their rotational behaviors. Unlike the case of a carbon substituent which exclusively rotates outward to furnish the corresponding *E*-butadiene, silyl, germyl, and stannyl substituents rotate in both inward and outward directions to afford a mixture of *Z*- and *E*-butadienes. The order of inward preference is Si > Sn > Ge.<sup>19</sup> The rotational behaviors of silyl, germyl, and stannyl substituents can be accounted for by assuming donor/acceptor interaction between the HOMO and the  $\sigma^*$  orbital of group 14 elements. The three factors, *i.e.*, the energy level of the  $\sigma^*$  orbital, the spatial distribution of the  $\sigma^*$  orbital, and the interspatial distance between the  $\sigma^*$  orbital and HOMO are taken into account in interpreting the order of inward preference on qualitative basis.

Although it is well known that the  $\sigma^*$  orbital of carbon–group 14 elements has an electron accepting nature ( $\alpha$ -effect), there are few reports which compare a series of the 14 group elements.<sup>19</sup> The present study provides a new example for comparison of the substituent effect of the group 14 elements.

## Experimental

All manipulations were carried out with standard Schlenk techniques under a nitrogen atmosphere. Column chromatography was carried out on Wako gel C-200 (Wako). <sup>1</sup>H NMR Spectra were recorded on a Varian Gemini 2000 (300 MHz). <sup>13</sup>C NMR spectra were recorded on a Varian Gemini 2000 at 75 MHz. Proton chemical shifts were referenced to residual solvent signals in CDCl<sub>3</sub> ( $\delta$  7.26). Carbon chemical shifts were referenced to the deuterated solvent signals in CDCl<sub>3</sub> ( $\delta$  77.00). All reagents and solvents were used as obtained from commercial suppliers without further purification.



### 3-(1,1-Dimethylheptyl)cyclobutanone 2

To a mixture of Zn–Cu (4.63 g, 70.8 mmol) and 3,3-dimethylnon-1-ene (3.64 g, 23.6 mmol) in Et<sub>2</sub>O (48 mL) was added a solution of trichloroacetyl chloride (5.26 mL, 47.2 mmol) in 1,2-dimethoxyethane (24 mL) dropwise at room temperature. After being stirred for 2 days at room temperature, the mixture was filtered with Celite® (Et<sub>2</sub>O), and the filtrate was washed successively with H<sub>2</sub>O, saturated NaHCO<sub>3</sub> solution and brine. The organic layer was dried over MgSO<sub>4</sub> and concentrated. The residue was purified by column chromatography on silica gel (hexane:AcOEt = 20:1) to give 2,2-dichloro-3-(dimethylheptyl)cyclobutanone (5.41 g) as a yellow oil.

To a mixture of cyclobutanone and Zn–Cu (6.70 g, 102.5 mmol) and in THF (50 mL) was added water (5 mL) dropwise at 0 °C. After being stirred for overnight at room temperature, the mixture was filtered with Celite® (Et<sub>2</sub>O), and the filtrate was washed with 1 N HCl, saturated NaCl solution (two times) and dried over MgSO<sub>4</sub>. The solvents was evaporated, and the residue was purified by Kugelrohr distillation (0.8 mmHg, 100–110 °C) to afford 3-(dimethylheptyl)cyclobutanone **2** (2.53 g, 12.7 mmol, 54% in 2 steps). <sup>1</sup>H NMR (CDCl<sub>3</sub>, 300 MHz) δ 0.85–0.89 (m, 9H), 1.23–1.25 (m, 10H), 2.32 (quint, *J* = 8.4 Hz, 1H), 2.85 (d, *J* = 8.1 Hz, 4H). <sup>13</sup>C NMR (CDCl<sub>3</sub>, 75 MHz) δ 14.1, 22.7, 23.0, 24.0, 30.2, 31.9, 33.7, 33.8, 40.9, 47.4, 208.3. HRMS (CI) Calcd for C<sub>13</sub>H<sub>25</sub>O (MH<sup>+</sup>): 197.1905. Found: 197.1903.

### 3-(1,1-Dimethylheptyl)cyclobutene 3

A solution of 3-(dimethylphenylsilyl)cyclobutanone **2** (2.53 g, 12.7 mmol) in ethanol (16 mL) was added dropwise to a suspension of *p*-tosylhydrazine (2.36 g, 12.7 mmol) in ethanol (16 mL) at room temperature. Within 30 min the tosylhydrazone began to precipitate. Ethanol was removed under reduced pressure to afford hydrazone.

To a mixture of the hydrazone and N,N,N',N'- tetramethylethylenediamine (4.7 mL) in hexane (47 mL) was added *n*-BuLi (1.56 M in hexane, 17.9 mL, 27.9 mmol) dropwise at –78 °C, and then the mixture was allowed to warm gradually to room temperature. After being stirred overnight, the mixture was quenched with water at –78 °C, added 1 N HCl, and extracted with Et<sub>2</sub>O. The organic layer was washed with saturated NaHCO<sub>3</sub> aqueous solution and saturated NaCl solution, dried over MgSO<sub>4</sub>, and concentrated. The residue was purified by column chromatography on silica gel (hexane) to afford **3** (0.87 g, 4.82 mmol, 38%). <sup>1</sup>H NMR (CDCl<sub>3</sub>, 300 MHz) δ 0.80 (s, 3H), 0.82 (s, 3H), 0.88 (t, *J* = 6.8 Hz, 3H), 1.21–1.30 (m, 10H), 2.24 (d, *J* = 14.3 Hz, 1H), 2.38 (dd, *J* = 13.5, 4.3 Hz, 1H), 2.72–2.74 (m, 1H), 6.02 (dd, *J* = 2.7, 0.9 Hz, 1H), 6.07 (dd, *J* = 2.7, 0.9 Hz, 1H). <sup>13</sup>C NMR (CDCl<sub>3</sub>, 75 MHz) δ 14.2, 22.8, 23.1, 23.6, 24.2, 30.5, 31.9, 32.0, 33.6, 40.9, 54.2, 135.5, 138.9. HRMS (EI) Calcd for C<sub>13</sub>H<sub>24</sub> (M<sup>+</sup>): 180.1878. Found: 180.1879. Anal. Calcd for C<sub>13</sub>H<sub>24</sub>: C, 86.59; H, 13.41%. Found: C, 86.62; H, 13.69%.

### 3-Tributylstannylcyclobutene 6

To a solution of 3-(dimethylphenylsilyl)cyclobut-1-ene **4** (1.43 g, 7.6 mmol) in CH<sub>2</sub>Cl<sub>2</sub> (25 mL) was added slowly SnCl<sub>4</sub> (0.98 mL, 8.4 mmol) at –78 °C. After stirring overnight at room temperature, the solvent was removed under reduced pressure and the residue

was dissolved in THF (22 mL). To the mixture was added *n*-butylmagnesium chloride (2.0 M in THF, 21.5 mL, 43.0 mmol) at –78 °C. After being stirred at room temperature for 3 h, hexane was added and the resulting precipitate was filtered off. The filtrate was evaporated and the residue was passed through a short pad of silica gel. After evaporation, the residue was purified by silica gel column chromatography (hexane as an eluent) to afford **6** (0.86 g, 2.52 mmol, 33%). <sup>1</sup>H NMR (CDCl<sub>3</sub>, 300 MHz) δ 0.73–0.95 (m, 16H), 1.24–1.37 (m, 7H), 1.43–1.54 (m, 6H), 2.61 (d, *J* = 14.1 Hz, 1H), 2.77 (d, *J* = 4.5 Hz, 1H), 2.91 (dd, *J* = 14.0, 4.4 Hz, 1H), 5.80–5.81 (m, 1H), 6.18 (m, 1H). <sup>13</sup>C NMR (CDCl<sub>3</sub>, 75 MHz) δ 8.2, 13.3, 27.0, 28.8, 31.1, 35.9, 130.4, 141.5. HRMS (FAB) Calcd for C<sub>12</sub>H<sub>24</sub>Sn (M<sup>+</sup>–H): 344.1526. Found: 344.1454.

### Synthesis of the metal electrophiles

**Chlorodimethylhexylsilane.** To a solution of dichlorodimethylsilane (6.0 mL, 50.0 mmol) in Et<sub>2</sub>O (40 mL) was added dropwise *n*-hexylmagnesium bromide, prepared from 1-bromohexane (8.4 mL, 60.0 mmol) and Mg (1.82 g, 74.9 mmol) in THF (60 mL) at 0 °C. After stirring at room temperature for 3 h, hexane was added to the reaction mixture, and the resulting precipitate was filtered off. After evaporation of the volatile materials, the residue was purified by Kugelrohr distillation (16 mmHg, 71 °C) to afford chlorodimethylhexylsilane (1.50 g, 8.39 mmol, 17%). <sup>1</sup>H NMR (CDCl<sub>3</sub>, 300 MHz) δ 0.40 (s, 6H), 0.79–0.84 (m, 2H), 0.86–0.91 (t, *J* = 6.8 Hz, 3H), 1.29–1.41 (m, 8H). <sup>13</sup>C NMR (CDCl<sub>3</sub>, 75 MHz) δ 1.7, 14.1, 19.0, 22.6, 23.0, 31.5, 32.7.

### Chlorodimethylhexylgermane

To a solution of *n*-hexylmagnesium bromide prepared from 1-bromohexane (3.13 g, 19.0 mmol) and Mg (0.54 g, 22.2 mmol) in THF (19 mL) was added chlorotrimethylgermane (2.00 g, 13.0 mmol) at 0 °C. After stirring at room temperature for 12 h, the reaction mixture was quenched with saturated aqueous NH<sub>4</sub>Cl solution and extracted with Et<sub>2</sub>O. The combined organic layer was washed with saturated NaCl solution, dried over MgSO<sub>4</sub> and evaporated. The residue was purified by Kugelrohr distillation (30 mmHg, 110 °C) to afford hexyltrimethylgermane (1.94 g, 9.58 mmol). A mixture of hexyltrimethylgermane, SnCl<sub>4</sub> (1.1 mL, 9.58 mmol) and acetyl chloride (9.6 mL) was stirred at 60 °C for 4 h. After evaporation of the volatile materials, the residue was purified by Kugelrohr distillation (20 mmHg, 110 °C) to afford chlorodimethylhexylgermane (0.71 g, 3.16 mmol, 17%). <sup>1</sup>H NMR (CDCl<sub>3</sub>, 300 MHz) δ 0.67 (s, 6H), 0.89 (t, *J* = 6.8 Hz, 3H), 1.15–1.20 (m, 2H), 1.26–1.37 (m, 6H), 1.45–1.53 (m, 2H). <sup>13</sup>C NMR (CDCl<sub>3</sub>, 75 MHz) δ 3.4, 14.1, 21.7, 22.5, 23.9, 31.4, 32.2.

### Chlorodimethylhexyltin

To a solution of *n*-hexylmagnesium bromide, prepared from 1-bromohexane (3.54 g, 21.0 mmol) and Mg (0.68 g, 28.0 mmol) in THF (20 mL) was added trimethyltin chloride (1.0 M in THF, 14.5 mL, 14.5 mmol) at 0 °C. After stirring at room temperature for 8 h, the reaction mixture was quenched with H<sub>2</sub>O and extracted with hexane. The combined organic layer was washed with 2 N HCl solution and saturated NaCl solution, dried over MgSO<sub>4</sub> and evaporated. The residue was purified by Kugelrohr distillation (27 mmHg, 110 °C) to afford hexyltrimethyltin (4.05 g,

16.3 mmol). A mixture of hexyltrimethyltin and trimethyltin chloride (3.89 g, 19.5 mmol) was stirred at room temperature for 2 weeks. The mixture was subjected to Kugelrohr distillation (26 mmHg, 140 °C) to afford chlorodimethylhexyltin (2.46 g, 12.1 mmol, 58%). <sup>1</sup>H NMR (CDCl<sub>3</sub>, 300 MHz) δ 0.62 (s, 6H), 0.88 (t, *J* = 6.8 Hz, 3H), 1.25–1.36 (m, 8H), 1.62–1.69 (m, 2H). <sup>13</sup>C NMR (CDCl<sub>3</sub>, 75 MHz) δ –1.8, 14.1, 18.9, 22.5, 25.4, 31.3, 33.2.

### Synthesis of cyclobutenes having a substituent of group 14 elements

**3-(Dimethylhexylsilyl)cyclobutene 7.** To a solution of **6** (421 mg, 1.23 mmol) in THF (5 mL) was added *n*-BuLi (0.87 mL) at –78 °C. After stirring at –78 °C for 1 h, chlorodimethylhexylsilane (241 mg, 1.35 mmol) was added and stirred at –78 °C for 2 h then at room temperature overnight. The mixture was quenched with H<sub>2</sub>O at 0 °C, extracted with Et<sub>2</sub>O, dried over MgSO<sub>4</sub>, and concentrated. The residue was purified by column chromatography (hexane as an eluent) and GPC to afford **7** (147 mg, 0.75 mmol, 61%). <sup>1</sup>H NMR (CDCl<sub>3</sub>, 300 MHz) δ –0.060 (s, 3H), –0.055 (s, 3H), 0.51 (t, *J* = 7.8 Hz, 2H), 0.88 (t, *J* = 6.8 Hz, 3H), 1.26–1.32 (m, 8H), 2.31–2.39 (m, 2H), 2.63–2.69 (m, 1H), 5.95–5.97 (m, 1H), 6.04–6.06 (m, 1H). <sup>13</sup>C NMR (CDCl<sub>3</sub>, 75 MHz) δ –5.2, –5.1, 14.2, 14.5, 22.7, 24.0, 31.7, 32.4, 33.4, 34.1, 133.7, 139.0. HRMS (EI) Calcd for C<sub>12</sub>H<sub>24</sub>Si (M<sup>+</sup>): 196.1647. Found: 196.1648. Anal. Calcd for C<sub>12</sub>H<sub>24</sub>Si: C, 73.38; H, 12.32%. Found: C, 73.15; H, 12.58%.

**3-(Dimethylhexylgermyl)cyclobutene 8.** To a solution of **6** (150 mg, 0.44 mmol) in THF (3 mL) was added *n*-BuLi (0.34 mL) at –78 °C. After stirring at –78 °C for 1 h, chlorodimethylhexylgermane (120 mg, 0.54 mmol) was added and stirred at –78 °C for 2 h then at room temperature overnight. The mixture was quenched with H<sub>2</sub>O at 0 °C, extracted with Et<sub>2</sub>O, dried over MgSO<sub>4</sub>, and concentrated. The residue was purified by column chromatography (hexane as an eluent) to afford **8** (36.9 mg, 0.15 mmol, 34%). <sup>1</sup>H NMR (CDCl<sub>3</sub>, 300 MHz) δ 0.06 (s, 6H), 0.70–0.75 (m, 2H), 0.88 (t, *J* = 6.6 Hz, 3H), 1.26–1.36 (m, 8H), 4.0–4.36 (d with unresolved coupling, *J* = 13.8 Hz, 1H), 2.57 (d, *J* = 4.2 Hz, 1H), 2.73 (dd, *J* = 14.0, 4.4 Hz, 1H), 5.93–5.94 (m, 1H), 6.06–6.07 (m, 1H). <sup>13</sup>C NMR (CDCl<sub>3</sub>, 75 MHz) δ –5.9, –5.8, 14.2, 14.8, 22.7, 25.2, 31.6, 33.1, 33.7, 34.6, 133.1, 139.8. HRMS (EI) Calcd for C<sub>12</sub>H<sub>24</sub>Ge (M<sup>+</sup>): 242.1090. Found: 242.1098. Anal. Calcd for C<sub>12</sub>H<sub>24</sub>Ge: C, 59.81; H, 10.04%. Found: C, 60.06; H, 10.10%.

**3-(Dimethylhexylstannyl)cyclobutene 9.** To a solution of **6** (356 mg, 1.04 mmol) in THF (5 mL) was added *n*-BuLi (0.87 mL, 1.35 mmol) at –78 °C. After being stirred for 1 h, chlorodimethylhexyltin (382 mg, 1.42 mmol) was added and stirred at –78 °C for 2 h then at room temperature overnight. The mixture was quenched with H<sub>2</sub>O at 0 °C, extracted with Et<sub>2</sub>O, dried over MgSO<sub>4</sub>, and concentrated. The residue was purified by column chromatography (hexane as an eluent) to afford **9** (183 mg, 0.64 mmol, 62%). <sup>1</sup>H NMR (CDCl<sub>3</sub>, 300 MHz) δ 0.02 (s, 6H), 0.84–0.91 (m, 5H), 1.24–1.33 (m, 6H), 1.46–1.53 (m, 2H), 2.54 (d, *J* = 12.9 Hz, 1H), 2.74 (d, *J* = 4.8 Hz, 1H), 2.90 (dd, *J* = 13.5, 4.8 Hz, 1H), 5.83–5.85 (m, 1H), 6.15–6.16 (m, 1H). <sup>13</sup>C NMR (CDCl<sub>3</sub>, 75 MHz) δ –12.3, –12.2, 10.3, 14.2, 22.7, 26.8, 31.49,

31.52, 36.0, 131.3, 141.5. HRMS (EI) Calcd for C<sub>12</sub>H<sub>24</sub>Sn (M<sup>+</sup>): 288.0900. Found 288.0908.

### General procedure for thermal ring-opening reaction.

Cyclobutenes **3** and **7–9** was dissolved in *p*-xylene-*d*<sub>10</sub>. The solution in an NMR tube was heated in a temperature-controlled oil bath at 120 °C. The reaction was intercepted at intervals, and the <sup>1</sup>H NMR spectrum was recorded. The conversion and the *Z/E* ratio of butadienes were determined on the basis of the <sup>1</sup>H NMR integrations of the vinylic protons of the reactants and products for **3**, and methyl proton on the element center for the other. The authentic *E*-butadienes **12**, **14** and **16** were synthesized independently by reaction of the corresponding metal electrophiles with buta-1,3-dien-1-yl lithium, which was generated in situ from (*E*)-1-bromobuta-1,3-diene and *t*-BuLi.

### (*E*)-5,5-Dimethylundeca-1,2-diene 10

<sup>1</sup>H NMR (CDCl<sub>3</sub>, 300 MHz) δ 0.86–0.90 (t, *J* = 6.8 Hz, 3H), 1.00 (s, 6H), 1.17–1.26 (m, 10H), 4.96 (d with unresolved coupling, *J* = 10.2 Hz, 1H), 5.11 (dd, *J* = 17.4, 1.8 Hz, 1H), 5.66 (d, *J* = 15.6 Hz, 1H), 5.96 (dd, *J* = 15.6, 10.5 Hz, 1H), 6.32 (ddd, *J* = 17.1, 10.2, 9.9 Hz, 1H). <sup>13</sup>C NMR (CDCl<sub>3</sub>, 75 MHz) δ 14.1, 22.7, 24.6, 27.1, 30.1, 31.9, 36.0, 43.2, 114.5, 126.7, 137.8, 145.5. HRMS (EI) Calcd for C<sub>13</sub>H<sub>24</sub> (M<sup>+</sup>): 180.1878. Found: 180.1877.

### (*E*)-1-(Dimethylhexylsilyl)buta-1,3-diene 12

<sup>1</sup>H NMR (CDCl<sub>3</sub>, 300 MHz) δ 0.06 (s, 6H), 0.54–0.57 (m, 2H), 0.85–0.92 (m, 3H), 1.24–1.32 (m, 8H), 5.11 (d with unresolved coupling, *J* = 9.6 Hz, 1H), 5.13 (d with unresolved coupling, *J* = 16.8 Hz, 1H), 5.86 (d, *J* = 18.0 Hz, 1H), 6.31 (dt, *J* = 9.6, 16.8, 1H), 6.48 (dd, *J* = 9.6, 18.0, 1H). <sup>13</sup>C NMR (CDCl<sub>3</sub>, 75 MHz) δ –3.1, 14.2, 15.6, 22.6, 23.8, 31.6, 33.3, 117.4, 134.0, 139.9, 144.8. HRMS (EI) Calcd for C<sub>12</sub>H<sub>24</sub>Si (M<sup>+</sup>): 196.1647. Found 196.1640.

### (*E*)-1-(Dimethylhexylgermyl)buta-1,3-diene 14

<sup>1</sup>H NMR (CDCl<sub>3</sub>, 300 MHz) δ 0.19 (s, 6H), 0.76–0.81 (m, 2H), 0.85–0.92 (m, 3H), 1.25–1.39 (m, 8H), 5.07 (d with unresolved coupling, *J* = 10.2 Hz, 1H), 5.18 (d with unresolved coupling, *J* = 16.8 Hz, 1H), 6.07 (d, *J* = 18.0 Hz, 1H), 6.30 (ddd, *J* = 16.8, 10.2, 9.6 Hz, 1H), 6.47 (dd, *J* = 18.0, 9.6 Hz, 1H). <sup>13</sup>C NMR (CDCl<sub>3</sub>, 75 MHz) δ –3.7, 14.2, 16.0, 22.6, 25.0, 31.6, 32.9, 116.6, 135.7, 139.4, 143.4. HRMS (EI) Calcd for C<sub>11</sub>H<sub>21</sub>Ge (M<sup>+</sup>–CH<sub>3</sub>): 227.0855. Found 227.0852.

### (*E*)-1-(Dimethylhexylstannyl)buta-1,3-diene 16

<sup>1</sup>H NMR (CDCl<sub>3</sub>, 300 MHz) δ 0.13 (s, 6H), 0.86–0.93 (m, 5H), 1.24–1.30 (m, 6H), 1.33–1.56 (m, 2H), 5.06 (d with unresolved coupling, *J* = 9.9 Hz, 1H), 5.17 (d with unresolved resolved coupling, *J* = 17.1 Hz, 1H), 6.29 (d, *J* = 18.6 Hz, 1H), 6.33 (ddd, *J* = 17.1, 9.9, 9.6 Hz, 1H), 6.53 (dd, *J* = 18.6, 9.9 Hz, 1H). <sup>13</sup>C NMR (CDCl<sub>3</sub>, 75 MHz) δ –10.8, 11.1, 14.2, 22.7, 26.6, 31.5, 33.7, 116.2, 135.0, 139.9, 147.1. HRMS (FAB) Calcd for C<sub>12</sub>H<sub>24</sub>Sn (M<sup>+</sup>): 288.0900. Found 288.0894.

## Acknowledgements

We would like to thank Dr Jun-ya Hasegawa (Department of Synthetic Chemistry and Biological Chemistry, Kyoto University) for discussion.

## References

- 1 R. B. Woodward, R. Hoffmann, *The Conservation of Orbital Symmetry*, Academic Press, New York, 1970.
- 2 (a) W. R. Dolbier, Jr., H. Koroniak, K. N. Houk and C. Sheu, *Acc. Chem. Res.*, 1996, **29**, 471; (b) W. Kirmse, N. G. Rondan and K. N. Houk, *J. Am. Chem. Soc.*, 1984, **106**, 7989; (c) N. G. Rondan and K. N. Houk, *J. Am. Chem. Soc.*, 1985, **107**, 2099; (d) W. R. Dolbier, Jr., H. Koroniak, D. J. Burton, A. R. Bailey, G. S. Shaw and S. W. Hansen, *J. Am. Chem. Soc.*, 1984, **106**, 1871; (e) K. Rudolf, D. C. Spellmeyer and K. N. Houk, *J. Org. Chem.*, 1987, **52**, 3708; (f) R. Hayes, S. Ingham, S. T. Saengchantara and T. W. Wallace, *Tetrahedron Lett.*, 1991, **32**, 2953; (g) S. Niwayama and K. N. Houk, *Tetrahedron Lett.*, 1992, **33**, 883; (h) C. W. Jefford, G. Bernardinelli, Y. Wang, D. C. Spellmeyer, A. Buda and K. N. Houk, *J. Am. Chem. Soc.*, 1992, **114**, 1157; (i) S. Niwayama and K. N. Houk, *Tetrahedron Lett.*, 1993, **34**, 1251; (j) S. Niwayama, Y. Wang and K. N. Houk, *Tetrahedron Lett.*, 1995, **36**, 6201.
- 3 (a) E. Gil-Av and J. Shabtai, *J. Org. Chem.*, 1964, **29**, 257; (b) H. M. Frey, *Trans. Faraday Soc.*, 1964, **60**, 83.
- 4 (a) M. Murakami, Y. Miyamoto and Y. Ito, *Angew. Chem., Int., Ed.*, 2001, **40**, 189; (b) M. Murakami, Y. Miyamoto and Y. Ito, *J. Am. Chem. Soc.*, 2001, **123**, 6441; (c) M. Murakami and M. Hasegawa, *Angew. Chem. Int. Ed.*, 2004, **43**, 4874; (d) M. Hasegawa and M. Murakami, *J. Org. Chem.*, 2007, **72**, 3764.
- 5 An analogous effect has been reported in the ring opening of oxetene: (a) M. Shindo, K. Matsumoto, S. Mori and K. Shishido, *J. Am. Chem. Soc.*, 2002, **124**, 6840; (b) S. Mori and M. Shindo, *Org. Lett.*, 2004, **6**, 3945.
- 6 A theoretical study by Houk *et al.* supported our interpretation: P. S. Lee, X. Zhang and K. N. Houk, *J. Am. Chem. Soc.*, 2003, **125**, 5072.
- 7 For a different explanation, assuming geminal  $\sigma$  bond participation, see: (a) Y. Naruse and S. Inagaki, *Chem. Lett.*, 2007, **7**, 820; (b) M. Yasui, Y. Naruse and S. Inagaki, *J. Org. Chem.*, 2004, **69**, 7246; (c) H. Ikeda, T. Kato and S. Inagaki, *Chem. Lett.*, 2001, **30**, 270 and references therein.
- 8 For a preliminary study on the rotational behavior of stannyl substituents, see: M. Murakami, M. Hasegawa and H. Igawa, *J. Org. Chem.*, 2004, **69**, 587.
- 9 J. C. Giordan and J. H. Moore, *J. Am. Chem. Soc.*, 1983, **105**, 6541.
- 10 M. Murakami, I. Usui, M. Hasegawa and T. Matsuda, *J. Am. Chem. Soc.*, 2005, **127**, 1366.
- 11 L. C. Dias, P. R. R. Meira and E. Ferreira, *Org. Lett.*, 1999, **1**, 1335.
- 12 Geometries and energies of ground states and the transition states of the ring-opening reactions of **17**–**19** were obtained by density functional calculations using the GAUSSIAN98 program (Revision A.11.4), M. J. Frisch, G. W. Trucks, H. B. Schlegel, G. E. Scuseria, M. A. Robb, J. R. Cheeseman, V. G. Zakrzewski, J. A. Montgomery, R. E. Stratmann, J. C. Burant, S. Dapprich, J. M. Millam, A. D. Daniels, K. N. Kudin, M. C. Strain, O. Farkas, J. Tomasi, V. Barone, M. Cossi, R. Cammi, B. Mennucci, C. Pomelli, C. Adamo, S. Clifford, J. Ochterski, G. A. Petersson, P. Y. Ayala, Q. Cui, K. Morokuma, D. K. Malick, A. D. Rabuck, K. Raghavachari, J. B. Foresman, J. Cioslowski, J. V. Ortiz, B. B. Stefanov, G. Liu, A. Liashenko, P. Piskorz, I. Komaromi, R. Gomperts, R. L. Martin, D. J. Fox, T. Keith, M. A. Al-Laham, C. Y. Peng, A. Nanayakkara, C. Gonzalez, M. Challacombe, P. M. W. Gill, B. G. Johnson, W. Chen, M. W. Wong, J. L. Andres, M. Head-Gordon, E. S. Replogle, J. A. Pople, Gaussian, Inc., Pittsburgh, PA, 1998.
- 13 The B3LYP hybrid functional with 6-311G(d,p) basis sets were used on all elements for the ring-opening reaction of **17** and of **18**. For the ring-opening reaction of **19**, LANL2DZ basis sets augmented by one polarization function on H and C were employed. The effective core potential with triple- $\zeta$  basis set plus p- and d-type polarizations functions was used for Sn. All geometries obtained here were fully optimized by the gradient methods, and all energies include zero-point energies. Frequency calculations verified that all the stable points are true local minima and all transition states have only one imaginary frequency.
- 14 The inward/outward energy difference for **19** is  $-0.64$  kcal/mol at the LANL2DZdp.
- 15 A. E. Reed, L. A. Curtiss and F. Weinhold, *Chem. Rev.*, 1988, **88**, 899.
- 16 E. D. Glendening, J. K. Bandenhop, A. E. Reed, J. E. Carpenter, F. Weinhold, *NBO Version 3.1*, Theoretical Chemistry Institute, University of Wisconsin, Madison, 1995.
- 17 (a) A. L. Allred and E. G. Rochow, *J. Inorg. Nucl. Chem.*, 1958, **5**, 264; (b) A. L. Allred, *J. Inorg. Nucl. Chem.*, 1961, **17**, 264; (c) L. C. Allen, *J. Am. Chem. Soc.*, 1989, **111**, 9003.
- 18 M. Shindo, K. Matsumoto and K. Sishido, *Tetrahedron*, 2007, **63**, 4271.
- 19 The same order in the magnitude of electron accepting effect of  $\sigma^*$  orbitals of group 14 elements was observed in metalloles. S. Yamaguchi, Y. Itami and K. Tamao, *Organometallics*, 1998, **17**, 4910.